

MODELLING THE BREAKING PROCESS OF TWISTED FIBRE BUNDLES AND YARNS

László M. VAS and Géza HALÁSZ

Department of Polymer Engineering and Textile Technology
Technical University of Budapest,
H-1521. Budapest, Hungary
Phone 463-1111

Received: October 17, 1994

Abstract

A brief description of a statistical modelling method is given to predict the total loading and breaking process of fibre bundles generated by the tensile test. Relationships between some normalized strength properties and the twist parameter of bundle, as well as the influence of the elastic part of the twist are examined by using the results of modelling an idealized structure of twisted fibre bundle. As an experimental study ring-spun and rotor-spun yarns are tested and their structure is analysed with the aid of comparing the measured and modelled breaking processes.

Keywords: yarn model, fibre bundle strength, twisted fibre bundle breaking process, elastic twist.

1. Introduction

The computer-aided systems for testing the fibres and yarns as well as designing the geometry of different textile products make it possible, moreover, require to study the relationships between the properties of partially ordered structures and their macrostructural strength in order to take them into consideration in planning structures built up of fibres or reinforced by fibres before manufacturing.

As well-known, there is a close relationship between the course of the load-elongation curve obtained by tensile tests and the structure in respect of the structural changes of textile products when elongating them gradually. In principle *Fig. 1* illustrates these changes. The front part of the curve ($O - A_2$) is related to the elongating process with stretching the fibres - most of them are slack here - and elongating the mostly well-ordered fibre bundle.

With the breakage of the first fibre the back part of the curve ($A_2 - F$), that is the breaking process begins and through additional breakages and slippages it goes on until the bundle is completely broken (point F) [4, 6].

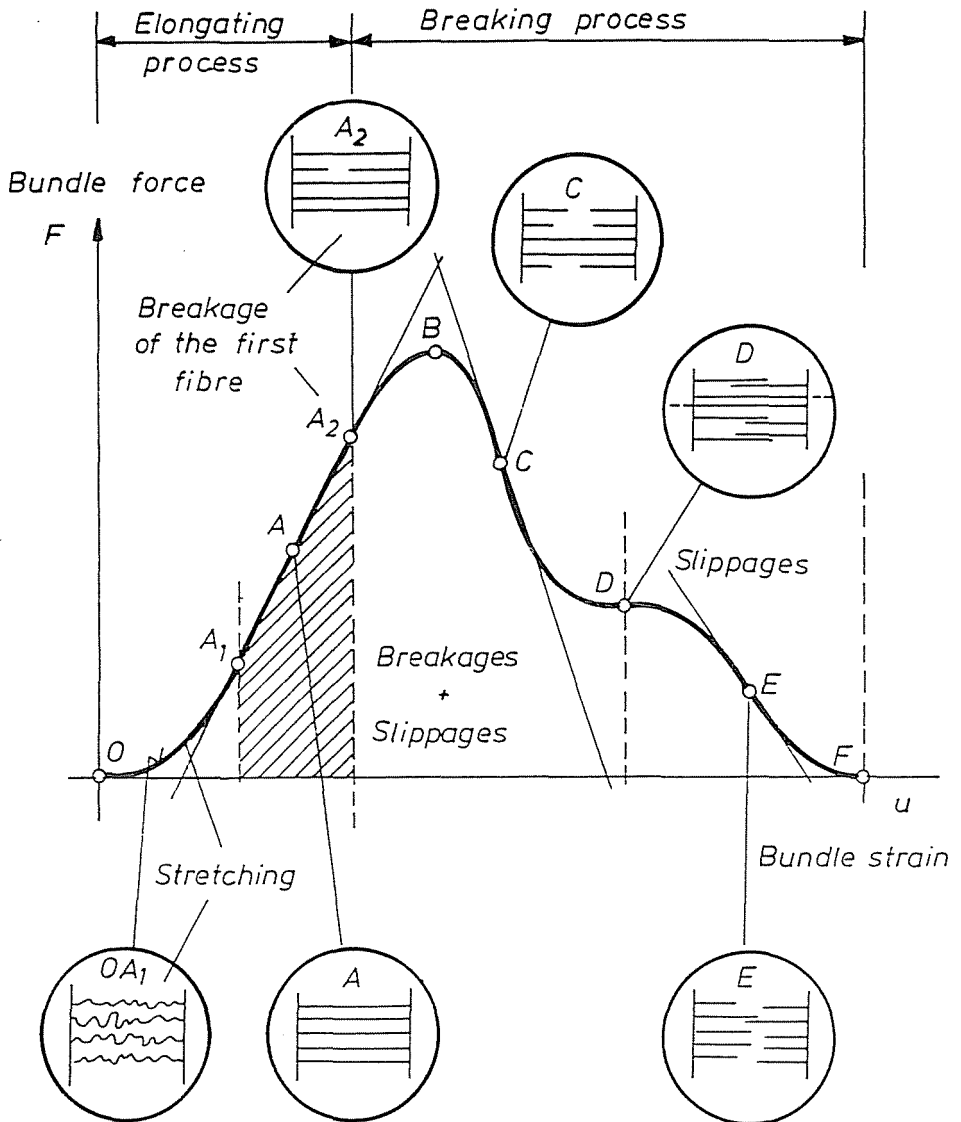


Fig. 1. The characteristic parts of a load-elongation curve obtained by tensile test

The aim of this paper is to show the results of the statistical modelling method and its use for analysing the tensile strength properties and the structure of twisted fibre bundles and yarns.

2. Fibre-bundle-cell Method

Fig. 2 shows the structural levels of twisted fibre bundles in the approach of the statistical modelling method mentioned above. Using the known geometrical and mechanical properties of the given fibres, a statistical single-fibre-model is defined, which is perfectly flexible and elastic but it breaks at a random value of load [9–12].

The model of flat bundle is built up of fibres independent of each other. In the real fibre bundles there can be well-ordered and amorphous parts. According to their arrangements within the bundle the fibres can be classified into subbundles or bundle-cells [9–12]:

- (1) Well-ordered bundle of normal fibres (*E*-bundle).
- (2) Preset bundle (*EH*-bundle), in which the fibres can be randomly preloaded or precrimped.
- (3) Slipping bundle (*ES*-bundle), in which the fibres may randomly break or slip out of the grips or of each other.

The model of the composite flat bundle is constructed of these bundle-cells connected pararely with chosen weight-ratios. The model structure of the twisted bundle like yarns is built up of composite flat bundles forming cylindrical layers after shearing them according to the twist angle required like the helix yarn model.

Fig. 3 shows the arrangement of a single fibre in a sheared flat bundle and a cylindrical layer of yarn. The tensile test of the bundle or yarn induces the elongation of fibre. The expression to calculate this strain e versus the bundle strain u from the fibre position is [10, 12]:

$$\varepsilon(u) = (1 + \epsilon_0) \left[\frac{(1 + u)^2 + \frac{e_0^2}{L_0^2}}{1 + p^2 \frac{e_0^2}{L_0^2}} \right]^{\frac{1}{2}} - 1, \quad (1)$$

where l_0 , ϵ_0 and e_0 , L_0 are the unloaded length, the initial strain before shearing, and the initial obliquity of fibre, the unloaded length of bundle after shearing. The factor $1 - p$ is related to the elastic strain caused by shearing the bundle. If $p = 1$, there is no strain of that kind. The formula (1) forms the basis of computing the tensile force in a single fibre using the real or an idealized relationship between strain and force, as well as the expected value of the bundle force utilizing the fact that all the parameters of fibre and bundle can be random variables with known probability distribution.

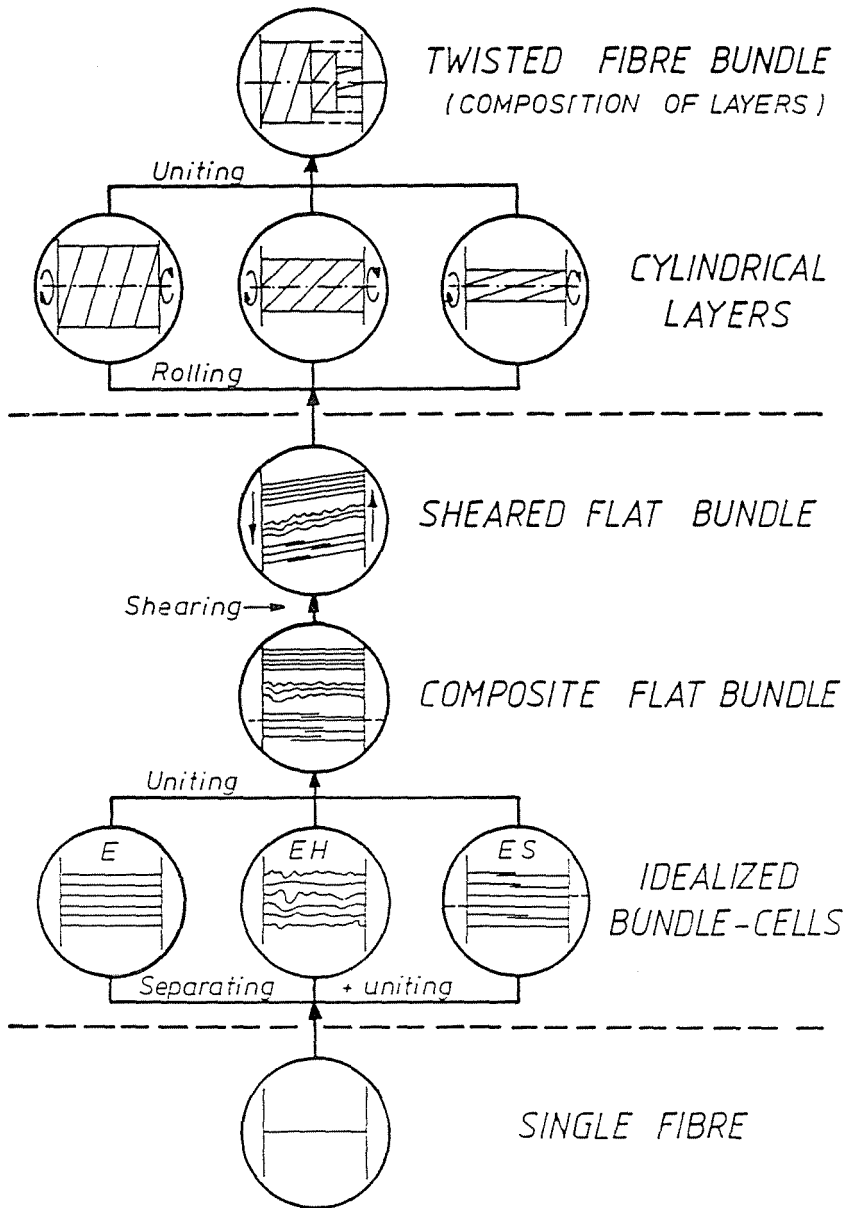


Fig. 2. The structural levels of twisted fibre bundles considered for the modelling method

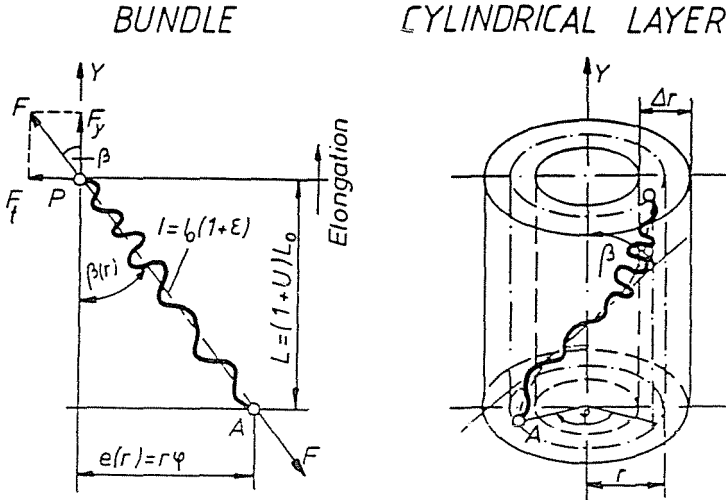


Fig. 3. The arrangement of a single fibre in a sheared flat bundle and a cylindrical layer of yarn

3. Idealized Fibre-bundle-cells

Assuming that the fibres have a linear stain-force relationship with random parameters like the breaking strain ϵ_B and the breaking force F_B , as well as they are gripped, in parallel Fig. 4 illustrates the properties of the three types of fibre-bundle-cells. These properties define the *E-bundle* of ideal gripping. The *EH-bundle* is a preset *E-bundle* and its fibres have a random initial strain ϵ_B . Preloading or precrimping means that $\epsilon_0 > 0$ or $\epsilon_0 < 0$. Because of the perfect flexibility, the fibre precrimped can not transmit force until uncrimping [9, 11].

Fibres of the *ES-bundle* can be gripped at both ends or they are parts of a fibre-chain in the bundle. Their gripping is not ideal that is why they can slip if the limit force of slippage (F_S) is smaller than the breaking force (F_B). Both the limit force and the length of slip page are random variables [9, 11].

To simplify the model, the probability distributions of all the random variables mentioned before are assumed to be normal. So, the expected value of the tensile force of the bundle-cells ($\mathcal{E}(F) = F$) can be calculated. Dividing the expected value by the mean breaking force of fibres, the so called normalized tensile force of bundle ($FH < 1$) can be computed and plotted as it is shown in Fig. 5 for the three fibrebundle-cells. In general, the maximum value of the normalized force course is called the utilization factor of fibre strength in bundle and denoted by *FH* here. The variable

■ IDEALIZED BUNDLE - CELLS

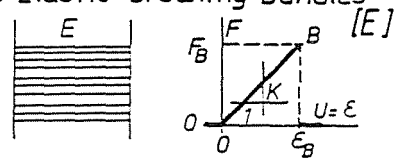
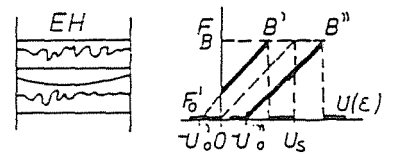
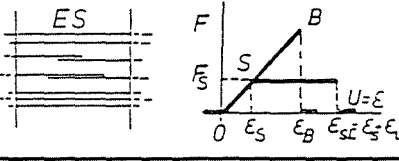
Type of bundle	Random parameters
<p>● Elastic-breaking bundles</p> 	<p>► Breaking</p> <p>strain $\epsilon_B > 0$</p> <p>force $F_B > 0$</p> <p>► Initial slope</p> <p>$K > 0$</p>
<p>● Preset E-bundle [EH]</p> 	<p>► Preloading: $\epsilon_0 > 0$</p> <p>Precrimping:</p> <p>$U = \frac{\epsilon - \epsilon_0}{1 + \epsilon_0} \quad \epsilon_0 < 0$</p>
<p>● Slipping E-bundle [ES]</p> 	<p>► Strain and force limit of slippage</p> <p>$\epsilon_s > 0, F_s > 0$</p> <p>► Relative slippage length</p> <p>$\epsilon_l > 0$</p>

Fig. 4. Properties of the idealized bundle-cells

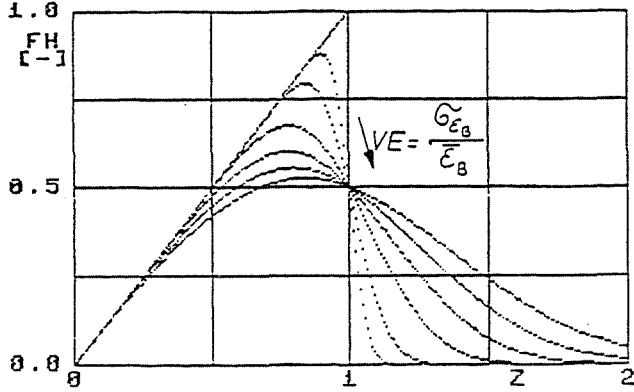
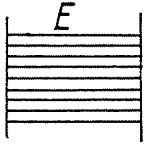
z in the diagrams is the bundle strain normalized by the mean breaking strain of fibres ($\bar{\epsilon}_B$).

The top diagram in Fig. 5 shows some normalized force-strain curves with different value of the variance of fibre breaking strain for the E -bundle ($VE = .05, .1, .2, .3, .4, .5$). These kinds of curves represent the best utilization of the fibre strength [9].

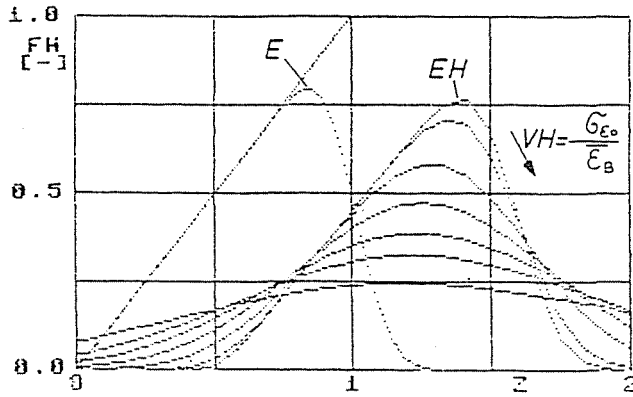
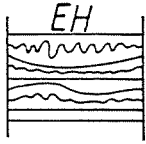
The diagram in the middle shows the force-strain curves of some EH -bundle calculated with the same mean value of precrimping ($EH = 0.5$) but with different variance of that ($VH = .05, .1, .2, .3, .5, .7$). Increasing that variance, the curve becomes flatter and at higher values the maximum slope will considerably decrease [9].

Some typical force-strain curves of the ES -bundle are shown in the bottom diagram, where the mean slippage strain (ES) and the mean slippage length (EL) vary receiving the very same values ($ES = EL = .1, .2,$

E-BUNDLE



EH-BUNDLE



ES-BUNDLE

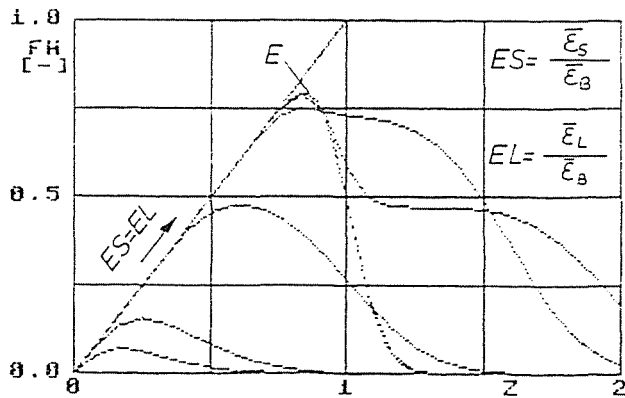
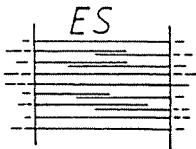


Fig. 5. Normalized force-strain curves of the idealized fibre bundle-cells

.5, .8, 1, 1.5). If they are small, then most fibres will slip. If the slippage strain is large that is greater than the breaking strain, the fibre breaking dominates the process. If they are near to the breaking strain value, then – as a result of slippages – a kind of plateau appears on the curve after the peak point [9].

It can be stated that the main types of changes in the structure and the course of the elongating and breaking process during the tensile test can be described by using the idealized bundle-cells above.

4. Modelling Twisted Fibre Bundles

Carrying out a tensile test of a twisted bundle or a yarn, the length of yarn increases and its diameter decreases (*Fig. 6*). This effect can be considered by using the contraction function shown in *Fig. 6* on the left side below. The contraction exponent α is equal to the Poisson's ratio of yarn if the strain of yarn (u) is small. In the case of that kind of contraction function, the volume of the tested bundle (\mathcal{V}) will increase in function of the bundle strain u when $\alpha > 0.5$ and decrease when $\alpha < 0.5$, while $\alpha = 0.5$ means the constant volume, it behaves like rubber. Here, it is assumed that the yarn segment is short enough to consider it approximately a piece of filament yarn, furthermore, it is made by twisting an E -bundle. It means that a kind of statistical helix yarn model can be used. The expected value of the tensile force for such a twisted fibre bundle can be calculated by integrating the fibre forces with respect to the helix radius (r) and the number of fibres or the filling density in the helix layer (ξ) [10, 12]:

$$FH(u; R_0, T) = \frac{1}{\bar{F}_B A_f(R)} \int_0^R \mathcal{E}(F_y(u, r, r_0, T)) dA_f(r), \quad (2)$$

where the cross sectional area of fibres in the helix layer:

$$dA_f(r) = \xi(r) 2r \pi dr$$

and F_y is the fibre force projected into the yarn axis direction y .

Fig. 7 shows the variation of fibre strain in twisted bundle as a function of bundle strain. The twist parameter of the helix layer with radius r in the unloaded bundle is denoted by $g_0 = g_0(r_0) = 2\pi r_0 T$, while by $TG = g_0(R_0)$ on the surface of twisted bundle. It is easy to see that by a given contraction exponent α , there is a critical value of the twist parameter that is the tangent of the twist angle β :

$$TG = \tan \beta = (\alpha)^{\frac{-1}{2}} \quad (3)$$

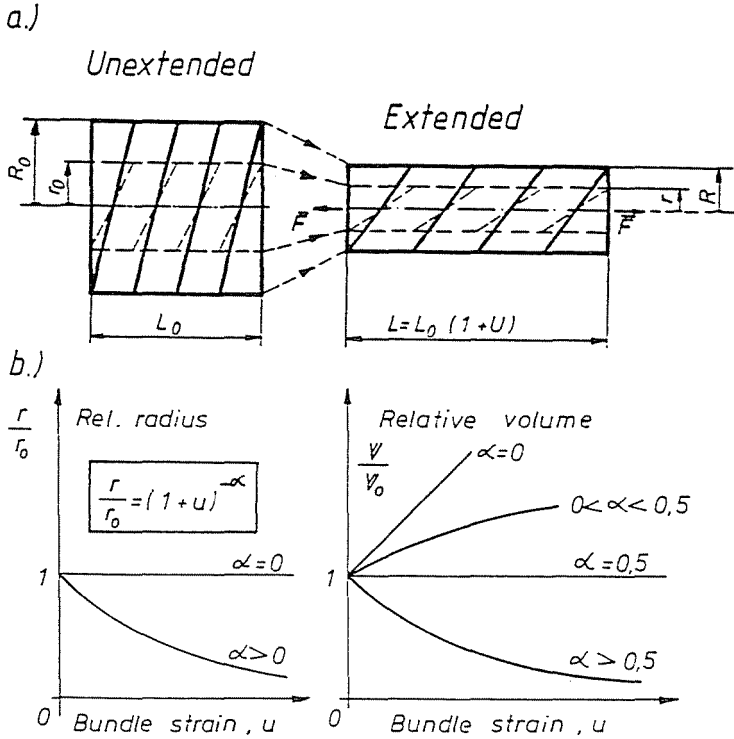


Fig. 6. a) Decrease of diameter with extending a yarn specimen; b) Contraction function of yarn assumed for modelling

that when $TG > (\alpha)^{-1/2}$, then the fibres in the layer outside will be slack, in an interval of u determined by α and TG (Fig. 7).

Fig. 8 illustrates the tensile force – bundle strain curves of different yarn models where the filling density of yarn is uniform. In order to show the basic characteristic of the elongating and the breaking processes, the variance of the fibre breaking strain was taken at a very small value: $VE = V = 0.5\%$. The family parameter of the curves is the twist parameter TG . For the diagrams a) b) c) the contraction exponents are in order 0, 1, and the critical value is $\alpha = TG$. Diagram d), as a special case, shows the curves of an untwisted yarn segment, which means a kind of limitation for the decrease of volume while increasing the bundle strain u .

For the twisted fibre structure models described above, Fig. 9 shows the variation of the three main properties characterizing the elongating and breaking processes as a function of the twist parameter:

- The utilization factor of fibre strength (FH) (Diagram a);

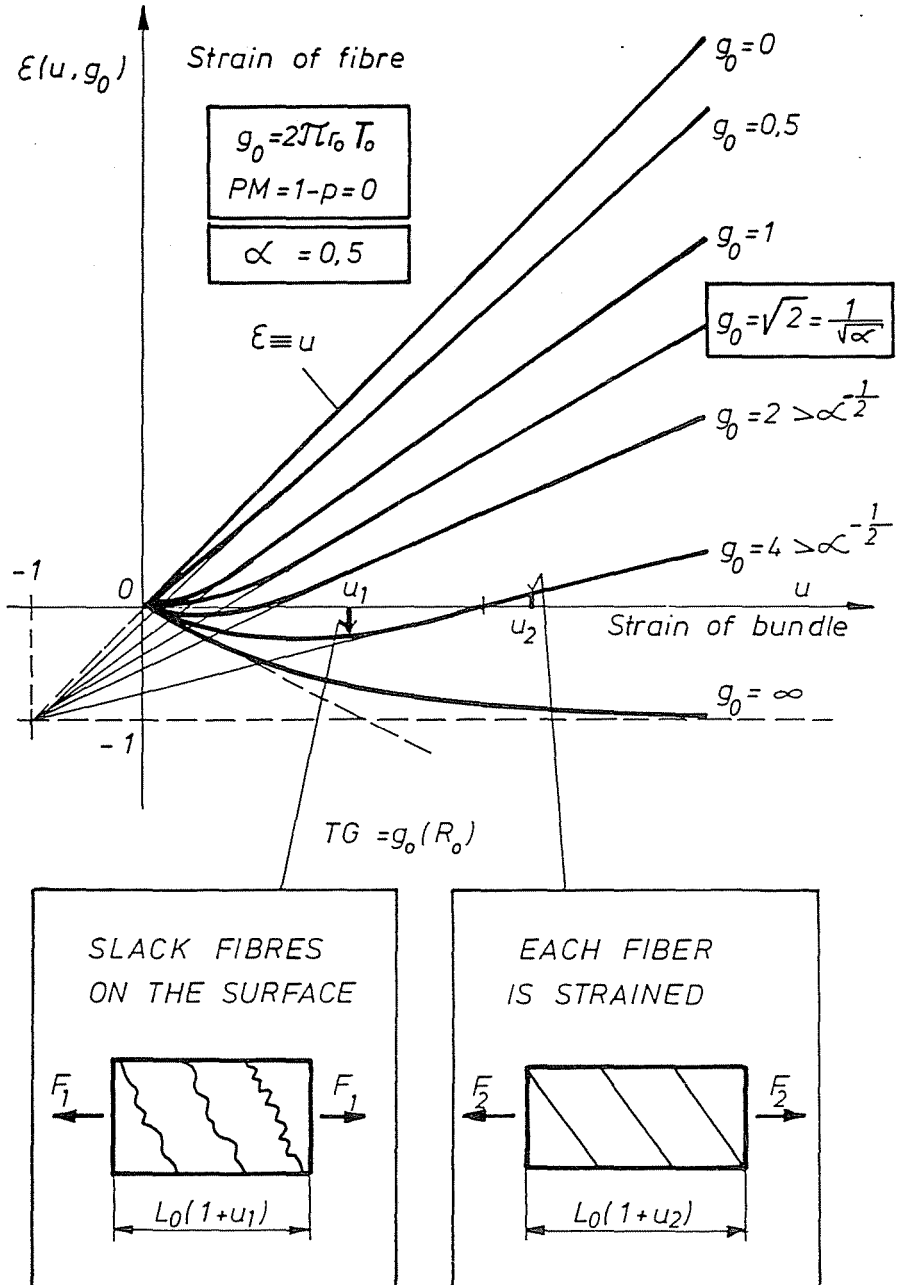


Fig. 7. The variation of the fibre strain in twisted bundle with the bundle strain

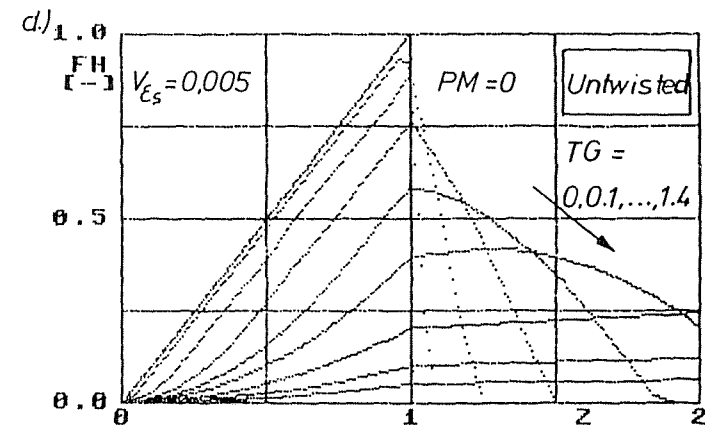
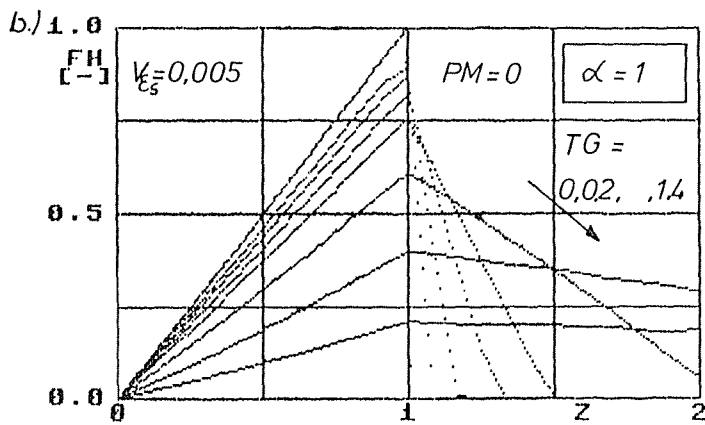
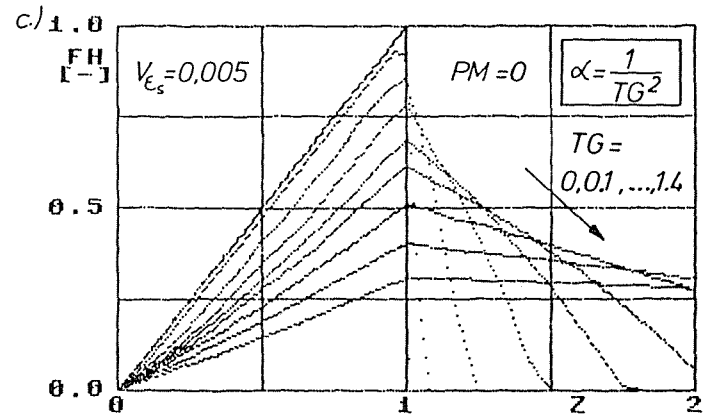
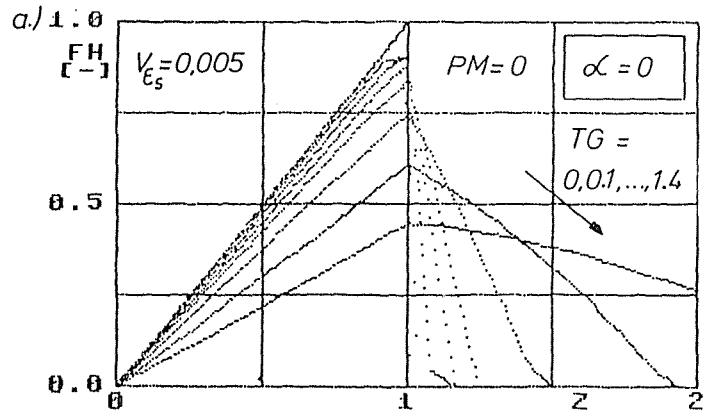


Fig. 8. Calculated bundle strain curves of different yarn models

- The maximum slope DF (Diagram *b*) which means a kind of utilization factor of fibre initial rigidity;
- The strain of bundle at the peak point (z) like a kind of breaking strain of bundle.

Increasing the value of the twist parameter or the contraction exponent, the utilization factors decrease while the strain z increases.

5. Influence of the Elastic Twist

The twisted bundles examined above were free of remaining stress. However, in practice the yarn often contains some elastic strain remained in the fibres after twisting. Assuming that the elastic part of the twist is given by the factor $PM = 1 - p$ (see expression (1)), *Fig. 10.a* illustrates the distribution of fibre strain along the diameter of twisted bundle where the curves above each other concern increasing values of the bundle strain u .

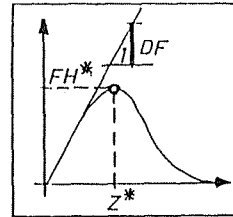
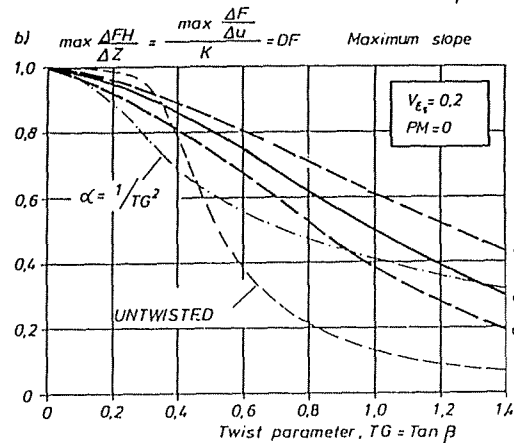
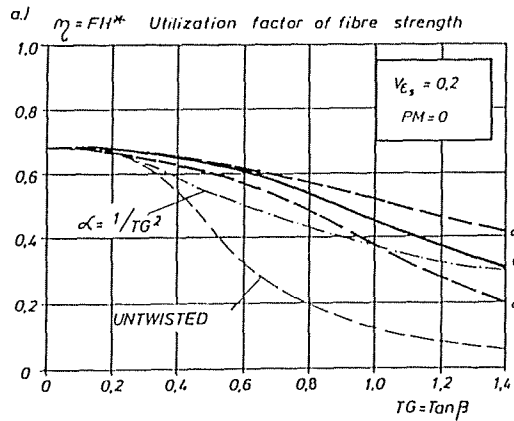
In the initial state ($u = 0$) that distribution is like a parabola convex from below. Suppose that the fibres do not break yet, the large enough bundle strain can compensate it and the distribution becomes concave from below. Between them the uniform distribution appears as well, as a borderline case. This is illustrated by the diagrams in *Fig. 10 b*, which are calculated and plotted by modelling.

The diagrams in *Fig. 11* show the variation of the utilization factor of fibre strength versus the twist parameter, as well as the factor of the elastic strain. It can be found that the existence of the not too high elastic strain can improve the utilization of fibre strength when the twist parameter is not too small. In *Fig. 11* ($\alpha = 0.5$), it is realized when $0.05 < PM < 0.15$ and $TG > 0.6$.

6. Experimental Study and Comparison

To demonstrate the applicability of the analytical models, two yarns, a 67%-33% polyester-cotton ring-spun yarn and a 100% cotton rotor-spun yarn were tested, modelled and analyzed. The yarns were made of the same cotton fibres. The fibres were taken out of the yarns after untwisting. *Fig. 12* shows the relative frequency diagrams of the breaking strain, the breaking load and the initial tensile rigidity for the cotton and polyester fibres measured on 10 mm of length. *Table 1* contains the test data. To obtain a more precise value, the variance of fibre breaking strains was calculated without the outliers, as well.

The length of the tested yarn segments was 10 mm, too. The results of testing can be found in *Table 2*. *Fig. 13* shows the relative frequency



c.) Strain of bundle at the peak point

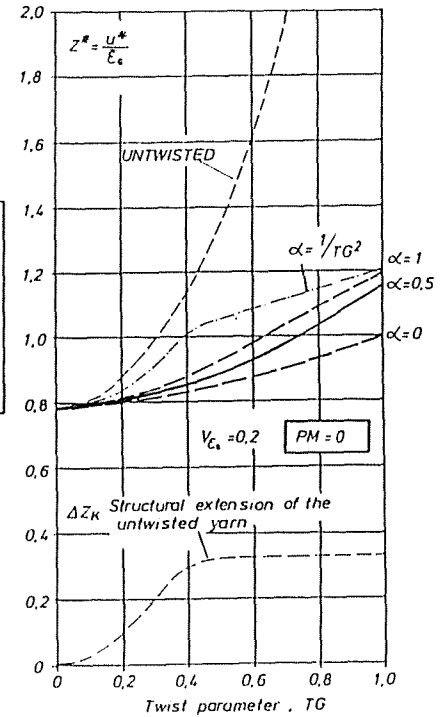


Fig. 9. Variation of the fibre strength utilization factor (a.), the relative maximum slope (b.), and the bundle strain at peak point (c.)

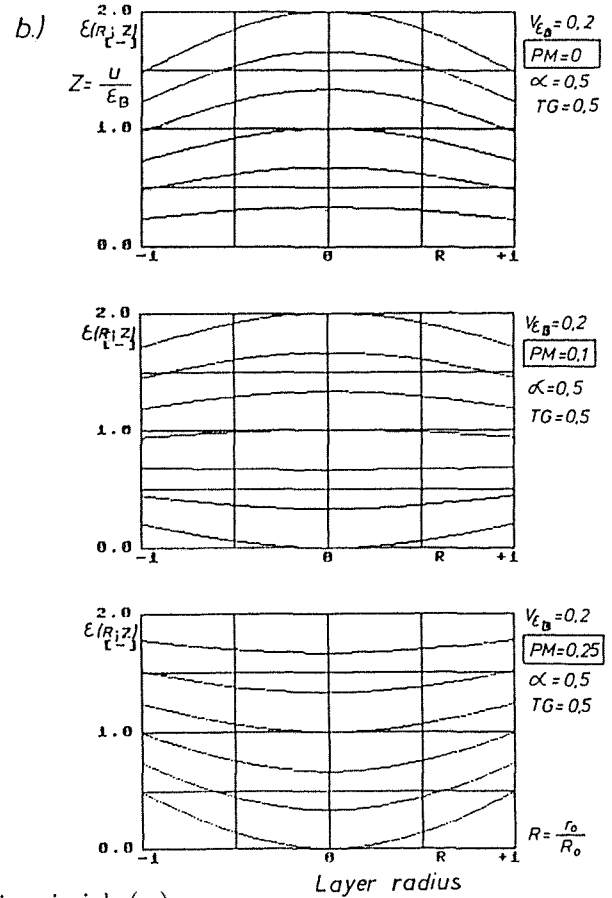
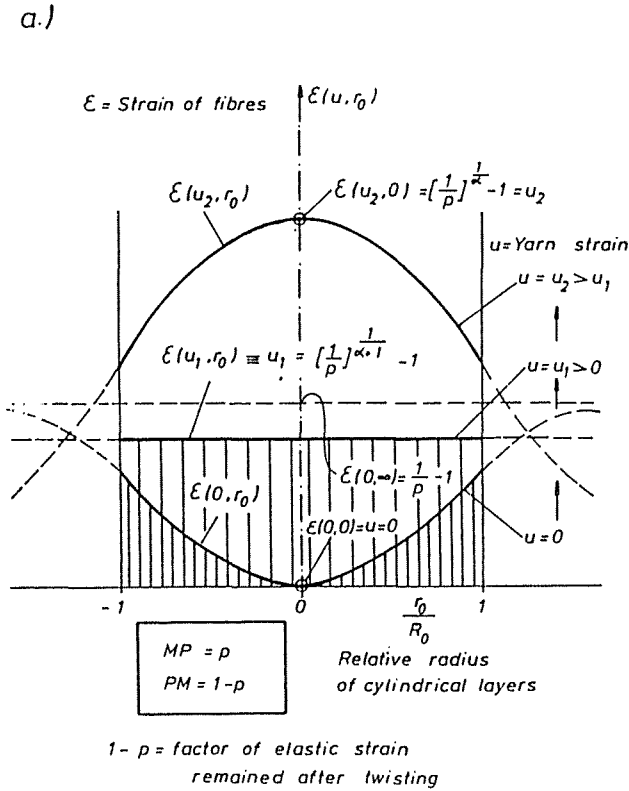


Fig. 10. Distribution of fibre strain in the bundle cross section in principle (a.) and modelled (b.)

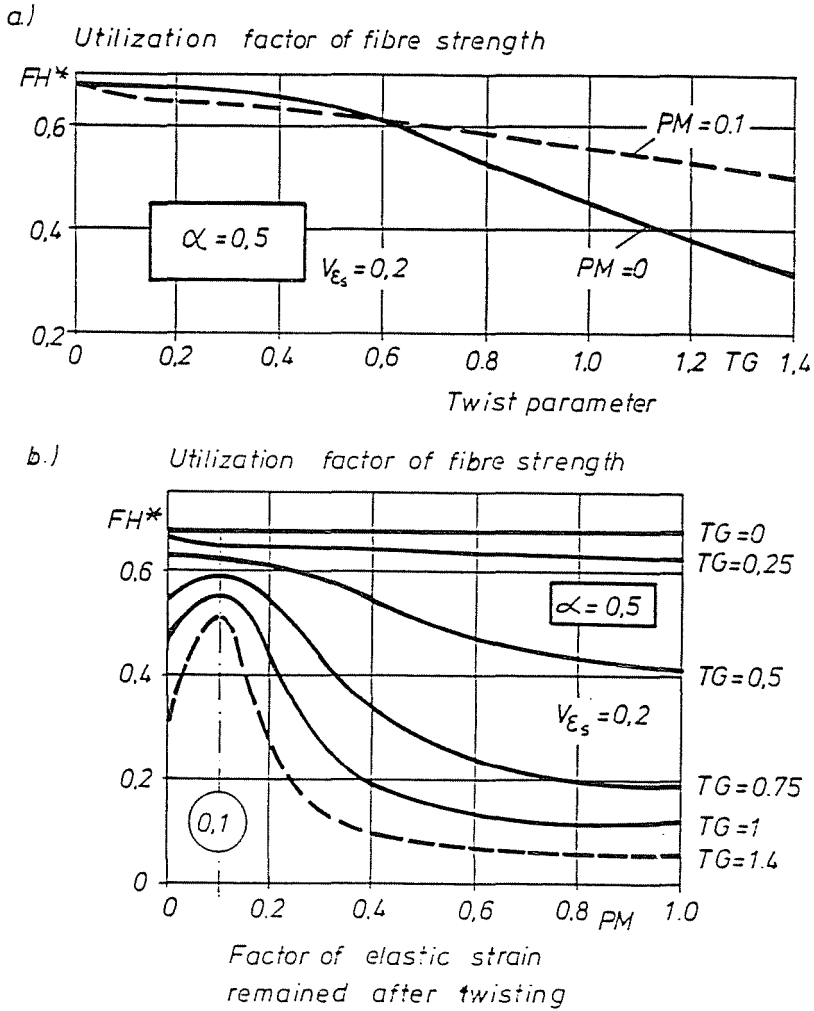


Fig. 11. Variation of the fibre strain utilization with the twist parameter (a.) and the factor of elastic strain

diagram and the empirical distribution function of the twist parameter TG and the factor of elastic twist PM , that are important data for modelling.

By using the data of yarn in Table 4 suitable models were created for both yarns as a first approach for iteration. The top diagrams in Fig. 14 illustrate the expected value curves of the tensile force modelled for both yarns and the bottom ones show the distributions of fibre strain in the yarn cross section. The difference between the behaviours of the two types of yarn can be well observed, which are also expressed by the very different contraction exponents chosen by fitting: $\alpha = 0.5$ for the ring-spun yarn

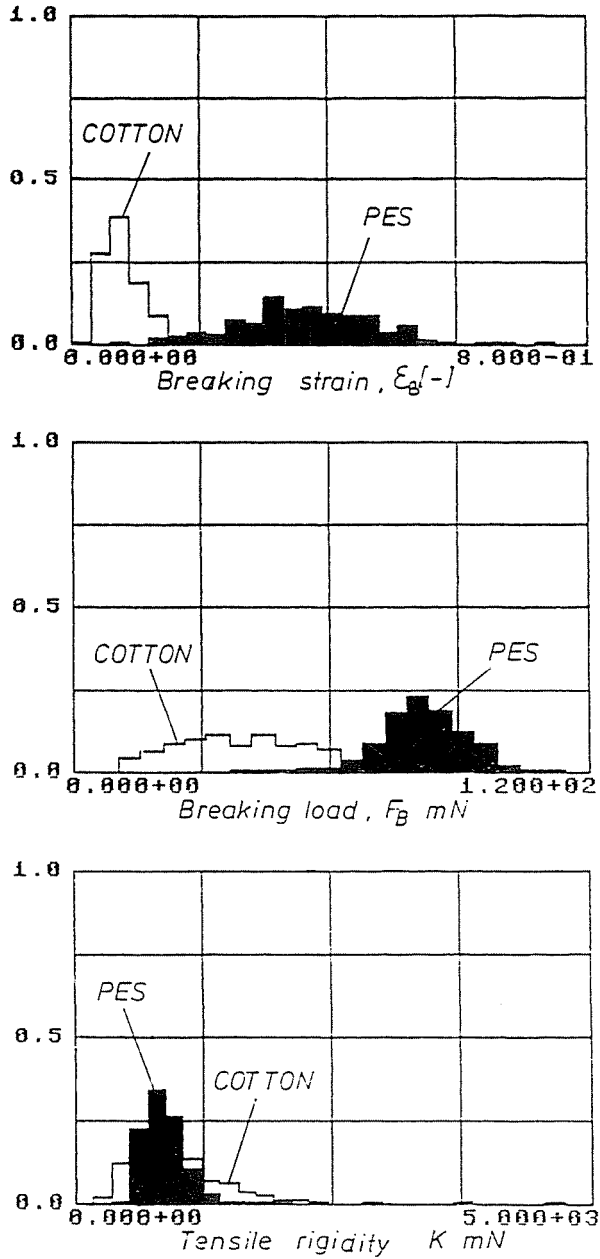


Fig. 12. Relative frequency diagrams of the tensile properties of the cotton and polyester (PES) fibres

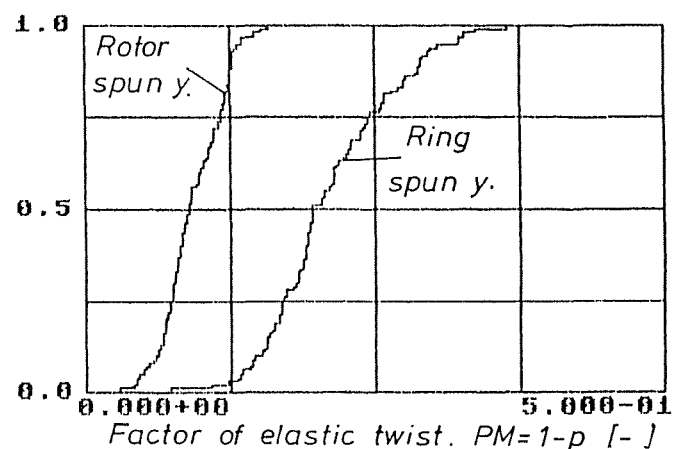
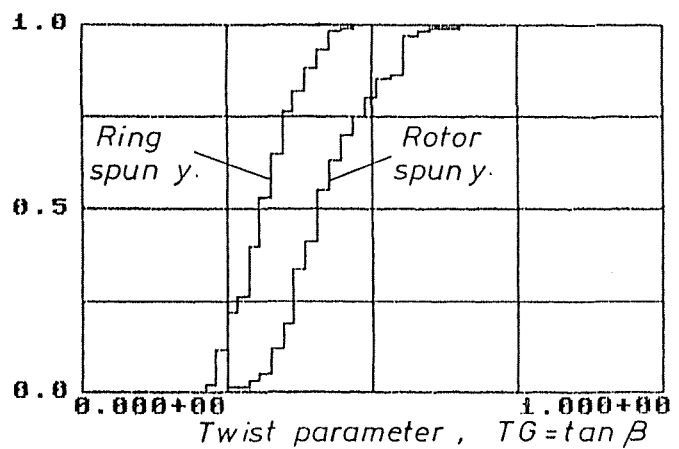
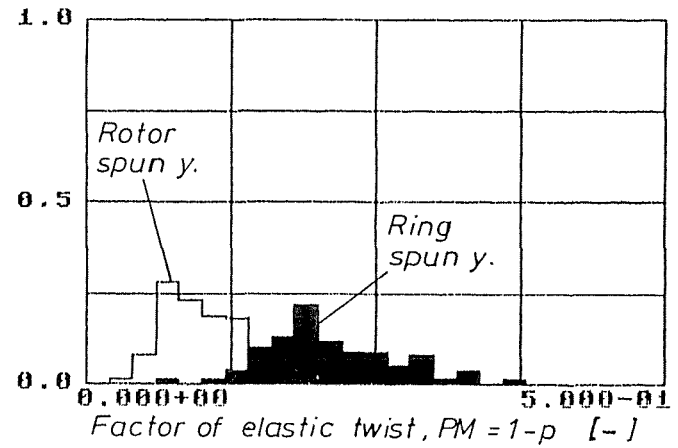
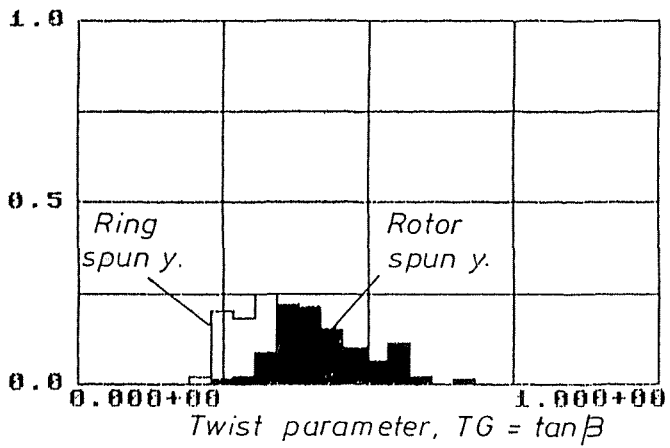


Fig. 13. Relative frequency diagram and empirical distribution function of the twist parameter and the elastic twist factor measured on yarns

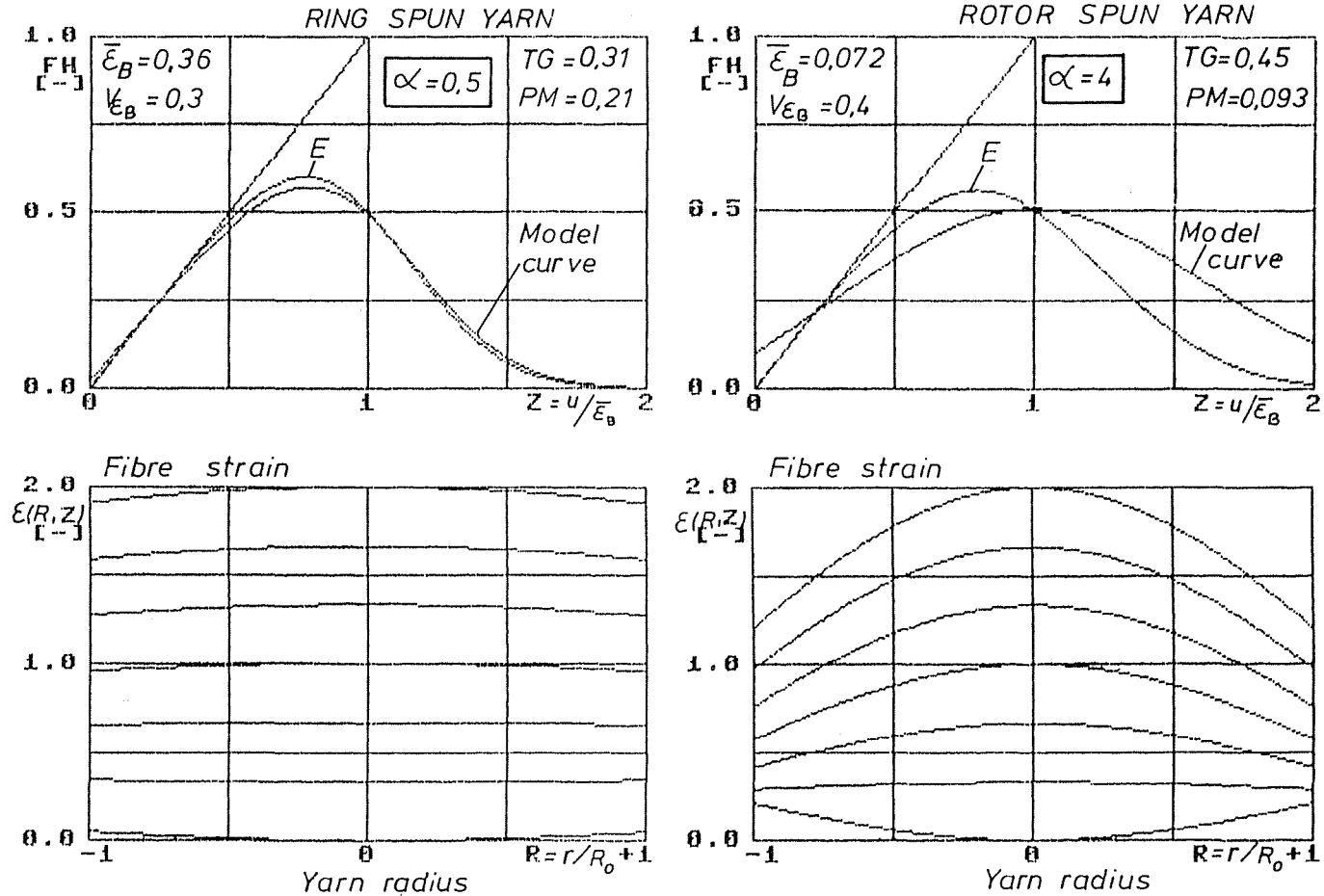


Fig. 14. Normalized bundle force-strain and fibre strain curves modelled for the tested yarns

Table 1
Test and calculated data of fibres

Fibre		Cotton (Co)	Polyester(PES)
Linear density		0.170 tex	0.168 tex
Upper mean length		32.5 mm	38 mm
Breaking load*	Mean	43.5 mN	81.3 mN
	CV%	42.5 %	12.8 %
Breaking strain*	Mean	0.078	0.362
	CV%	46.2 %	29.6 %
without outliers	Mean	0.072	0.358
	CV%	38.6 %	27.4 %
Initial tensile rigidity*	Mean	963 mN	873.5 mN
	CV%	59.2 %	40 %
Chord rigidity*	Mean	604 mN	224 mN

* Calculated from 200 measurements with 10 mm test length

Table 2
Test and calculated data of yarns

Yarn		Rotor-spun yarn	Ring-spun yarn
Blend ratios		Cotton 100%	PES 67%/Co 33%
Nominal linear density		29.4 tex	16.7 tex
Nominal twist rate		920 turns/m	900 turns/m
Linear density (q)*	Mean	27.1 tex	17.9 tex
	CV%	14.8 %	16.5 %
Diameter (D)*	Mean	0.219 mm	0.158 mm
	CV%	12.9 %	13.5 %
Twist angle (β)*	Mean	24.6	17.2
	CV%	17.5 %	13.1 %
Twist parameter (TG)* ($TG = \tan \beta$)	Mean	0.440	0.311
	CV%	9.1 %	4.3 %
Twist rate (T)* ($TG = \tan \beta / D\pi$)	Mean	655 turns/m	640 turns/m
	CV%	26.3 %	20.5 %
Factor of elastic twist ($PM = 1 - p$)**	Mean	0.093	0.211
	CV%	28.8 %	26.1 %
Breaking load (F_{ymax})*	Mean	2.86 N	4.01 N
	CV%	12.8 %	18.6 %
Breaking strain (ε_y)*	Mean	0.090	0.256
	CV%	17.3 %	18.3 %
Initial tensile rigidity (K_y)*	Mean	41.1 N	40.6 N
	CV%	19.6 %	19.2 %
Chord rigidity*	Mean	31.8 N	15.7 N

* Calculated from 512 measurements with 10 mm test length

** Calculated from 100 measurements with 10 mm test length

Table 3
Calculated data of yarns for modelling

Yarn	Rotor-spun yarn		Ring-spun yarn	
Ratios of fibres in yarn cross-section				
Blend ratios	Cotton: 100%		Cotton: 33% PES: 67%	
Modified ratios*	Cotton: 100%		Cotton: 23% PES: 77%	
Mean linear density of fibre blend (q_f)	0.170 tex		0.168 tex	
Mean number of fibres in yarn cross-section (N)	159.4		106.5	
Mean breaking load of fibre blend (\bar{F}_B)				
With blend ratios	43.5	mN	68.8	mN
With modifying	43.5	mN	72.6	mN
Mean initial tensile rigidity of fibre blend (\bar{K}_f)				
With blend ratios	963	mN	903	mN
With modifying	963	mN	894	mN
Mean chord rigidity of fibre blend				
With blend ratios	604	mN	349	mN
With modifying	604	mN	311	mN
Characterizing breaking strain of fibre blend (ε_B)				
Mean ($\varepsilon_B = AE$)	0.072		0.36	
CV% ($V_{\varepsilon_B} = VE$)	0.40		0.30	
Mean twist parameter (TG)				
$TG = \tan \beta$	0.458		0.310	
$TG = \tan \beta$	0.440		0.311	
$TG = D\pi T$	0.450		0.317	
Factor of elastic twist				
$PM = 1 - p$	0.093		0.211	
Calculated by weighting with mean fibre lengths (raw estimation)				

that is it behaves like rubber; $\alpha = 4$ for the rotor-spun yarn that is it has a kind of loose structure.

By using the test data measured on 10 mm length, the three main properties of yarn were computed as local yarn data (Table 4), which represent the fluctuation of not only the linear density but the structure, as well. Without averaging, Fig. 15 and 16 illustrate the dispersion of these local data comparing them with the expected value curves calculated by the first-approach-models. In the case of the ring-spun yarn, a good ap-

proximation can only be found for the fibre strength utilization, while the model curve passes along above the center of the dispersion region for the bundle strain and fibre rigidity utilization. In the case of the rotor-spun yarn, the model curves can be considered upper estimations for the utilizations of fibre strength and rigidity, and lower estimation for the bundle strain at peak point.

On the one hand, the differences found above can be explained by the fact that the expected values were calculated as a model with a well-determined structure without deviation in structure, therefore, we can calculate with a better fitting in comparing the mean values obtained by averaging the extensive test quantities like mass, volume and absolute twist (*Table 4*) with the values modelled. It is confirmed by the diagram in *Fig. 17 c*, where, besides the model curves, the deviation regions of the local yarn data are illustrated by ellipses, and small circles with central points show the values obtained by averaging extensive test data. These circles lie correctly under the idealized model curves. The diagrams in *Fig. 17* on the left side show the typical force-elongation curves of the fibres and yarns tested. The values of the fibre strength utilization calculated from the single measurements in *Fig. 17* fall into these small circles, as well.

On the other hand, the yarn segments tested are built up of not a single type of fibre bundle like the first-step-models applied, but at least of two different types according to *Figs. 17 a*, and *b*. Because of the single-fibre-bundle model, the validity of model extends essentially only to the narrow vicinity of the peak point *B*.

Since the ring-spun yarn consists of two types of fibres with different distributions of length, so the slippages of the short cotton fibres can modify mainly the rigidity DF and the strain z of bundle. The rotor-spun yarn can be considered a kind of core-sheath yarn, where the core is a well-ordered bundle with small twist and the sheath is a loose bundle with larger twist. In the case of both composite models, the decrease of the fibre strength utilization can be expected.

The application of the composite twisted bundles for modelling yarn is another step of the research to be carried on, so we have the intention to report on it in a next paper.

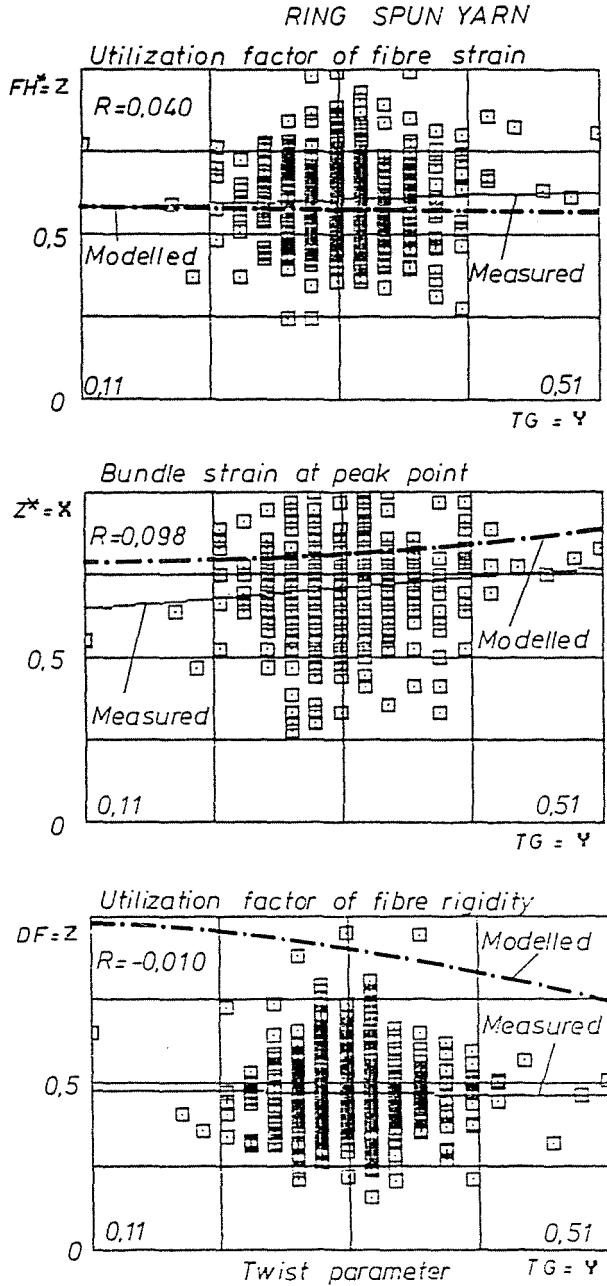


Fig. 15. The dispersion of the local tensile properties measured on the ring spun yarn and the global first-approach-model curves

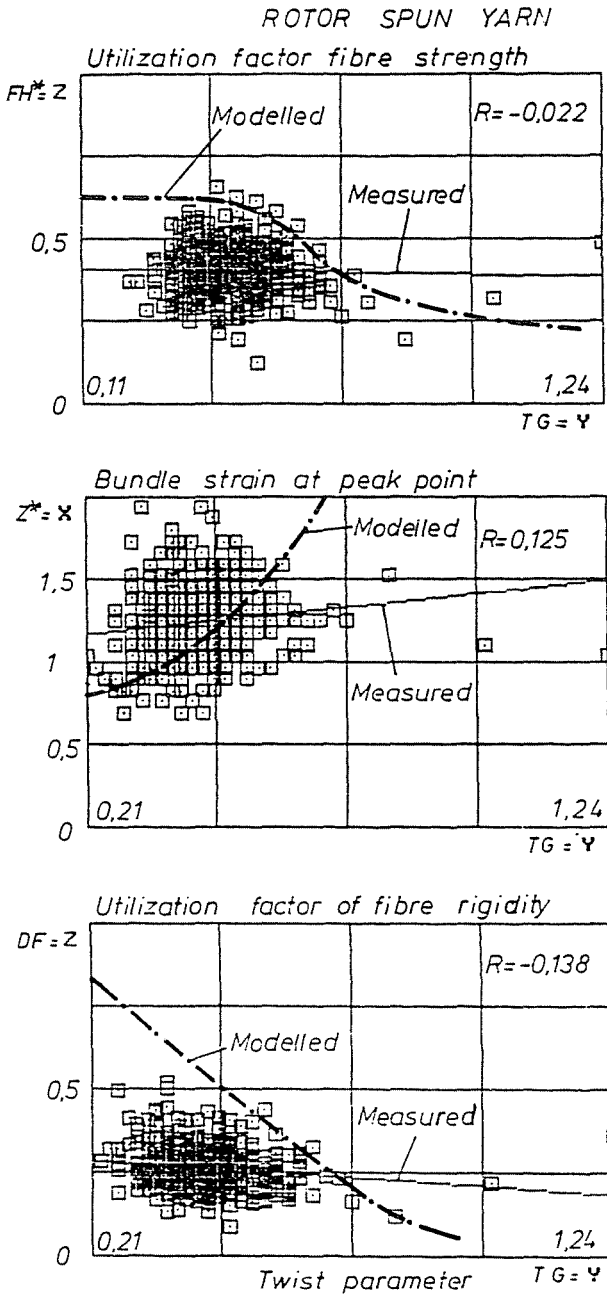


Fig. 16. The dispersion of the local tensile properties measured on the rotor spun yarn and the global first-approach-modell curves

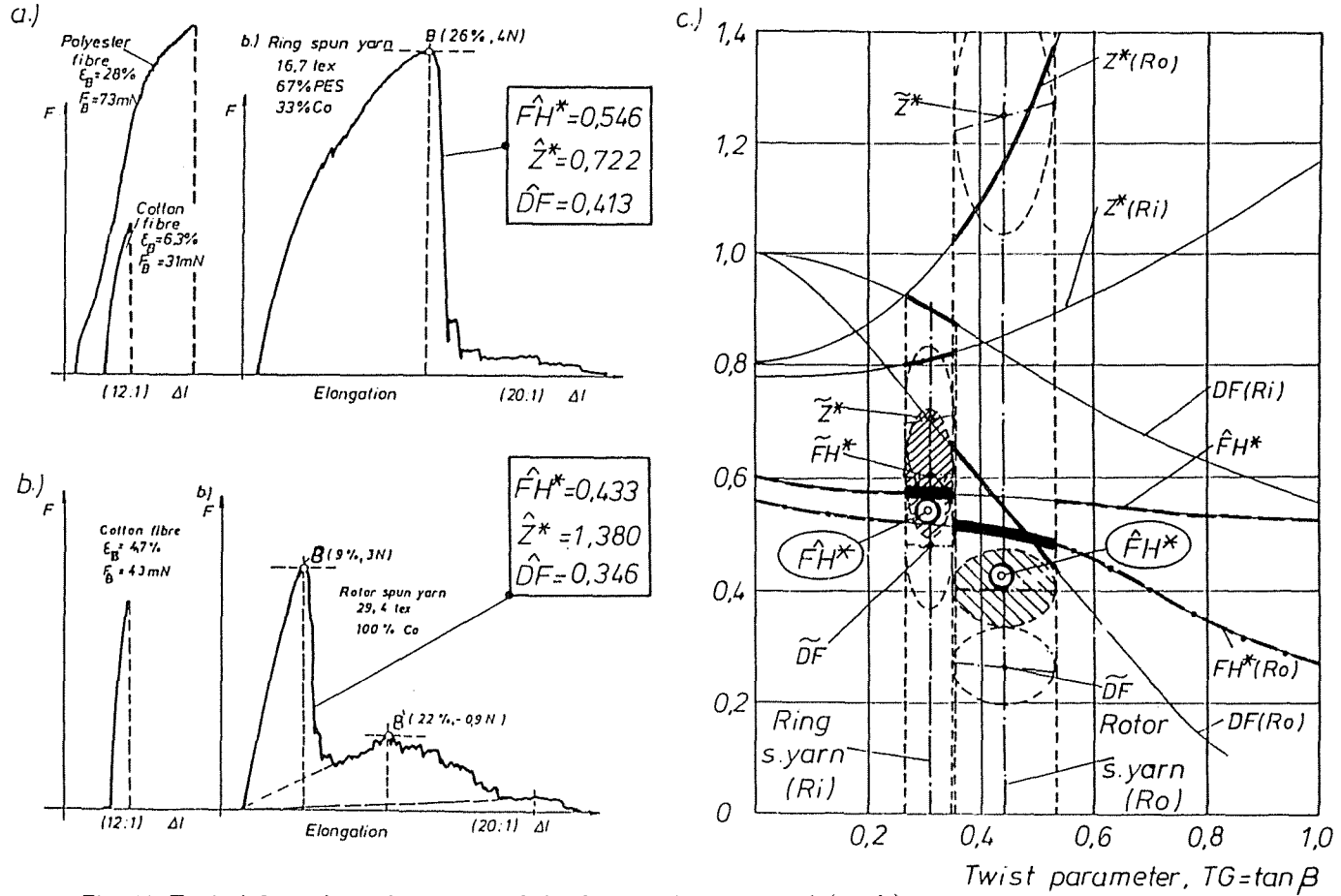


Fig. 17. Typical force-elongation curves of the fibres and yarns tested (a., b.) and the expected value curves of tensile properties calculated with de-

Table 4

Local and global data of yarns calculated from test data and obtained from modelling

Yarn		Rotor-spun yarn	Ring-spun yarn
Local utilization factor of fibre strength			
With blend ratios	Mean (FH^*)	0.403	0.608
	CV%	17.5 %	19.9 %
With modifying	Mean	0.403	0.576
Relative breaking strain			
	Mean (z^*)	1.252	0.712
	CV%	17.3 %	18.3 %
Local utilization factor of fibre tensile rigidity			
	Mean (DF)	0.261	0.473
	CV%	23.1 %	24.4 %
Global utilization factor of fibre strength			
With blend ratios	Mean (FH^*)	0.433	0.546
	Mean	0.433	0.517
Global utilization factor of fibre tensile rigidity			
With blend ratios	Mean (DF)	0.346	0.413
	Mean	0.346	0.463
Global utilization factor of fibre chord rigidity with blend ratios			
	Chord(yarn)/Chord(fibre)	0.330	0.421
	Initial(yarn)/Chord(fibre)	0.426	1.091
Yarn properties estimated by modelling			
Utilization factor of fibre strength			
	Mean (FH^*)	0.515	0.575
Relative breaking strain			
	Mean (z^*)	1.17	0.81
Utilization factor of tensile rigidity			
	Mean (DF)	0.54	0.90

7. Conclusion

This paper has attempted to model the twisted fibre bundle and analyse the relationships between strength properties and twist parameter, as well as factor of the elastic twist. It can be considered probable that there exists an optimum value of the elastic twist at which the fibre strength utilization takes up a maximum value. This phenomenon can be of importance for designing and manufacturing yarns.

The statistical modelling method was used to create twisted single-bundle models of real ring-spun and rotor-spun yarns as first- step models. The comparison of real yarn and model data has shown that both the yarn have complex structure, therefore, twisted composite bundle models are needed to describe them more precisely for the quantitative analysis and prediction.

8. Acknowledgements

The authors would like to express their thanks to the National Scientific Research Fund of Hungary for supporting the research reported here through grant OTKA 821.

References

1. PHOENIX, S. L.: Statistical Theory for Strength of Twisted Fibre Bundles with Applications to Yarns and Cables. *Textile Research Journal*, Vol. 49. No. 7. (pp 407-423). (July 1979)
2. DHAVAN, K. - BHATT, H. H. - RADHAKRISNAN, T.: Estimation of Tensile Properties of Single Cotton Fibers from Load- elongation Curves of Bundles. *Textile Research Journal* Vol. 54. No. 8. (pp 549-551). (Aug. 1984)
3. Zugprüfungen an Filamentgarnen. *Uster News Bulletin* Nr. 32 (S. 4-9). (Juli. 1984)
4. ZUREK, W.: The Structure of Yarn. Foreign Scientific Publications Department of the National Center for Scientific, Technical and Economic Information, Warsaw 1975.
5. NACHNE, R. P. - KRISHNA IYER, K. R.: Prediction of bundle strength from single-fiber test data. *Textile Research Journal* Vol. 50. (pp 639-641). (1980)
6. MORTON, W. E. - HEARLE, J. W. S.: Physical Properties of Textile Fibres. Chapter 4. The effects of variability. Manchester et London. The Textile Institute, Butterworths, 1962.
7. ZUREK, W. - FRYDRYCH, I. - KRUCINSKA, I.: The Fire Properties as Criteria of Yarn Quality. (In Hungarian) *Magyar Textiltechnika* Vol. 40. No. 12. pp. 611-617. (Dec. 1987)
8. BALOG I.: Study of the Relationship between the Local Geometrical and Strength Properties of Yarns. (In Hungarian) Diploma work. Budapest, 1991.
9. VAS L. M.: The Statistical Fibre Bundle Strength and its Application in Testing Fibres and Yarns. (In Hungarian) *Magyar Textiltechnika* Vol. 43. No. 4. pp. 165-185. (April 1990)
10. VAS L. M. - CSÁSZI F.: Application of the Part-fibre- Bundle Theory and Fibre Testing to Analysis of Cotton Yarns. *Proceedings of the 21st International Cotton Conference*, Bremen, pp. 249-268. 1992
11. VAS L. M.: Latest Results in the Tensile Test Theory of Fibre and Yarn Bundles Ordered into Plane. (In Hungarian) *Magyar Textiltechnika* Vol. 45. No. 3. pp. 71-75. (March 1992), No. 5-6. pp 137-142. (May-Jun. 1992), No. 7-8. pp 187-191. (July-Aug. 1992)
12. VAS L. M. - CSÁSZI F.: Use of the Composite-bundle Theory to Predict Tensile Properties of Yarns. *Journal of the Textile Institute* Vol. 84. No. 3. pp 448-463. (1993)